ChemPubSoc Europe

DOI: 10.1002/ejoc.201600158

EurJOC European Journal of Organic Chemistry

Full Paper

Macrocycles

Rotationally Restricted 1,1′-Bis(phenylethynyl)ferrocene Subunits in Macrocycles

Viktor Hoffmann,[a] Nicolas Jenny,[a] Daniel Häussinger,[a] Markus Neuburger,[a] and Marcel Mayor*[a,b,c]

Abstract: The synthesis of macrocycles comprising a 1,1′-bis(phenylethynyl)ferrocene subunit was developed to increase the structural control over the spatial arrangement of the two cyclopentadienyl ligands of the ferrocene junction. The target structures were obtained through a modular strategy that enables the assembly of varying ring sizes from a common precursor. In particular, macrocycles were either formed by an ether formation reaction or by ring-closing metathesis reactions. The macrocycles were obtained in reasonable isolated yields, which allowed their thorough characterization by one- and two-dimensional NMR spectroscopy experiments, and the identity of one macrocycle was corroborated by single-crystal X-ray diffraction.

Introduction

The astonishingly versatile organometallic compound ferrocene (Fc) is a prototype of its kind, first reported in 1951 by Pauson and Kealy.[1] Later, the structure was deduced on the basis of its reactivity to be an iron(II) ion caged by negatively charged cyclopentadienyl (Cp) ligands to form a sandwich-type motif.[2] Curiosity spurred rapid achievements in the study of its chemistry. Owing to its three-dimensional structure and its reversible one-electron redox behavior, Fc is ubiquitous in chemistry. For instance, 1,1′-bis(diphenylphosphanyl)ferrocene (DPPF) emerged as a very efficient and sterically adaptable phosphine chelate ligand in the palladium-catalyzed amination of aryl halides.[3] Unsymmetrically 1,3-disubstituted ferrocenes have drawn attention owing to their prospects for chiral electro-optical liquid-crystal devices,[4] and 1,1′-disubstituted phenylethynyl-linked ferrocene structures are considered as potential molecular wires.[5] A more everyday-life application is represented with the 1,1′,3-trisubstituted ferrocene derivative of lidocaine, which acts as a redox mediator between the glucose oxidase enzyme and an electrode to monitor glucose levels in the blood of people with diabetes.[6]

1,1′-Di(phenylene-ethynylene)ferrocene subunits were reported as redox-active subunits in molecular rods and have been contacted in molecular junctions.[7] Although the rotational freedom between both Cp units is usually an appealing feature of the ferrocene structure and has been used to construct the mechanical joints in scissor-type architectures,[8] this flexibility results in a large variety of possible conformations in molecular rods and, consequently, a poor structural control. To gain back the control over the spatial arrangement of the subunits, we became interested in integrating the 1,1′-di(phenylene-ethynylene)ferrocene subunit into a macrocyclic structure. Although the development of a suitable synthetic approach is the main focus of this report, a modular synthetic approach towards a second parallel bridging structure might even provide the tools to vary systematically the angle defined by both diphenylene-ethynylene subunits at the Fc junction.

Here, we report three macrocyclic model compounds **1**–**3** comprising 1,1′-di(phenylene-ethynylene)ferrocene subunits, as shown in Figure 1. Their syntheses are all based on ring-closing

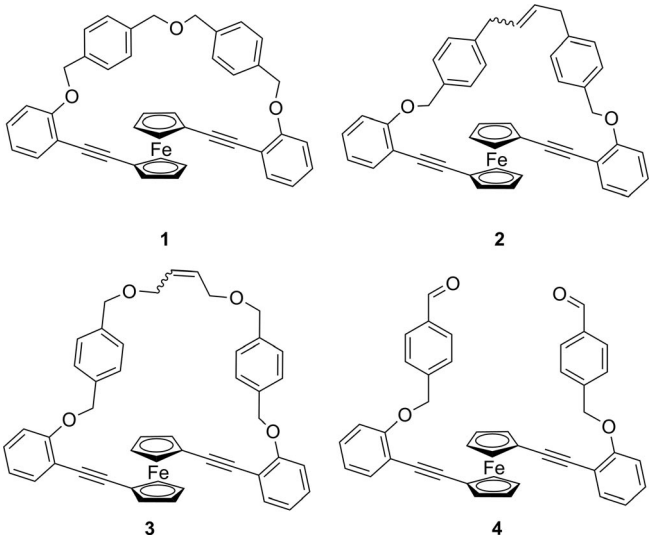

Figure 1. Macrocyclic model compounds **1**–**3** and their precursor **4**.

[a] *University of Basel, Department of Chemistry, St. Johanns-Ring 19, 4056 Basel, Switzerland*
E-mail: marcel.mayor@unibas.ch
http://www.chemie.unibas.ch/~mayor/index.html
[b] *Karlsruhe Institute of Technology (KIT), Institute of Nanotechnology (INT), P. O. Box 3640, 76021 Karlsruhe, Germany*
[c] *Lehn Institute of Functional Materials (LIFM), Sun Yat-Sen University, Guangzhou, P. R. China*

Supporting information for this article is available on the WWW under http://dx.doi.org/10.1002/ejoc.201600158.

reactions to form the second parallel bridge, and all three compounds have as a common precursor the parent 1,1′-di(phenylene-ethylene)ferrocene structure with oxybenzyl-4-benzaldehyde substituents at the *ortho* positions of the phenylene rings on both sides (**4**). Thanks to the intramolecular nature of the ring-closing reaction, these macrocycles were formed in acceptable yields of 57 to 70 % and were isolated in excellent purity by chromatography.

Synthetic Strategy

The closing of a macrocycle is usually a late step in a synthetic strategy and is often performed under high-dilution or pseudo-high-dilution conditions to favor the desired intramolecular macrocyclization over intermolecular oligomer and polymer formation. Exceptions are synthetic strategies that use templates or particular prefolded precursors. Here, we considered two conceptually different strategies, namely, the "capping" approach and the "bridge-closing" strategy displayed in Scheme 1. Although the capping strategy appears to be considerably more appealing owing to the large variety of different bridging structures that could be introduced in a single step, we were exclusively successful with the bridge-closing strategy.

The bridge-closing strategy might also offer modular diversity in the bridging structure depending on the chemistry selected for the bridge formation. Particularly appealing would be an open-bridge intermediate (**D** in Scheme 1) with exposed functional groups that would give access to different types of coupling reactions to close the bridge. More important than the increased modularity in the bridging structure is the increased probability that a suitable reaction could be found to close the bridge. Guided by these rationales, we chose the benzylic aldehyde precursor **4**, which gives access to a broad variety of potential ring-closing reactions, as displayed in Scheme 2. The precursor **4** with two exposed benzaldehyde moieties could be closed directly through an intramolecular McMurry-type reaction catalyzed by a low-valent titanium species.[9]

Here, we focus on the reduction of the benzaldehyde moieties to benzylic alcohol moieties to give access to nucleophilic substitution chemistry, either to close the bridge with an ether-type bridge or to introduce low-molecular-weight extensions comprising alternative functional groups such as terminal olefins, which would offer ring-closing olefin metathesis (RCM) chemistry as promising bridging chemistry.

In an alternative approach, the bridge might also be closed by using suitable bifunctional small molecules, such as a bis-Wittig salt or a bis(amine) (R in Scheme 2). The first approach would result in a bis(olefin)-bridged macrocycle, whereas the second approach, upon double Schiff base formation, would close the bridge with a bis(imine) structure. The appealing feature of this strategy would again be its modularity, as it would, in principle, provide access to structures with various opening angles at the ferrocene joint through the introduction of bifunctional small molecules with various spacings between both functional groups.

Results and Discussion

As we were tempted by the promise of large modularity in the bridging motif, our initial attempts followed the "capping" strategy (Scheme 1). Thus, the symmetric 1,1′-functionalized ferrocene rod **9** with two phenol groups as potential nucleophiles to form bridges with various bis(halide) compounds was assembled. The synthesis of **9** is summarized in Scheme 3 and comprises the double Sonogashira cross-coupling of the unsymmetrical acetylene **6** and 1,1′-diiodoferrocene (**7**) as the key step. The required tetrahydropyran-protected (THP-protected) 2-ethynyl-5-(2′-triisopropylsilylethynyl)-4-methoxyphenol **6** was obtained by adapting an established procedure developed by Höger and co-workers,[10] which takes advantage of the chemo-

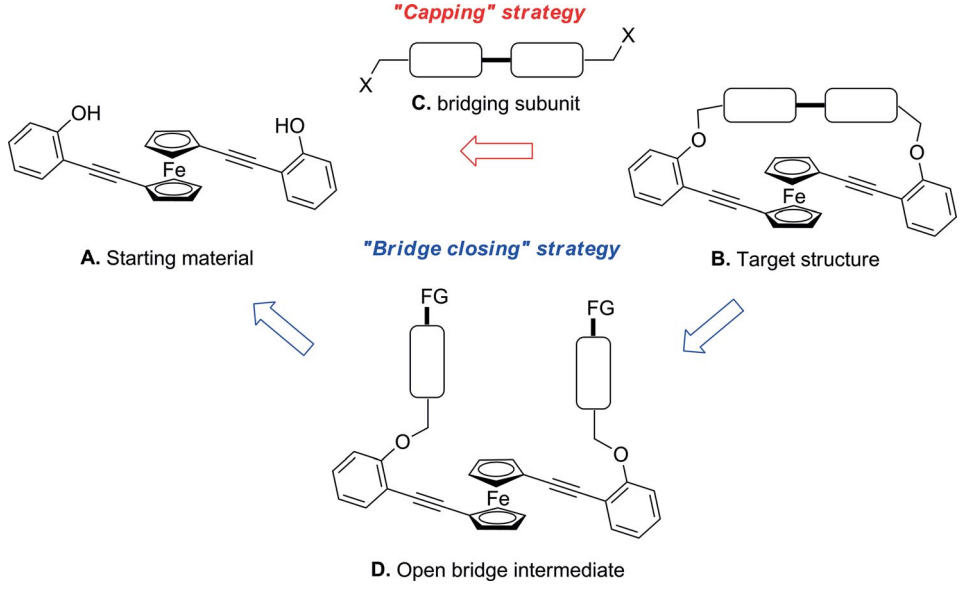

Scheme 1. Assembly of the 1,1′-di(phenylethynyl)ferrocene macrocycle through a disconnection approach following either the capping strategy (top: red arrow) or the bridge-closing strategy (bottom: blue arrows).

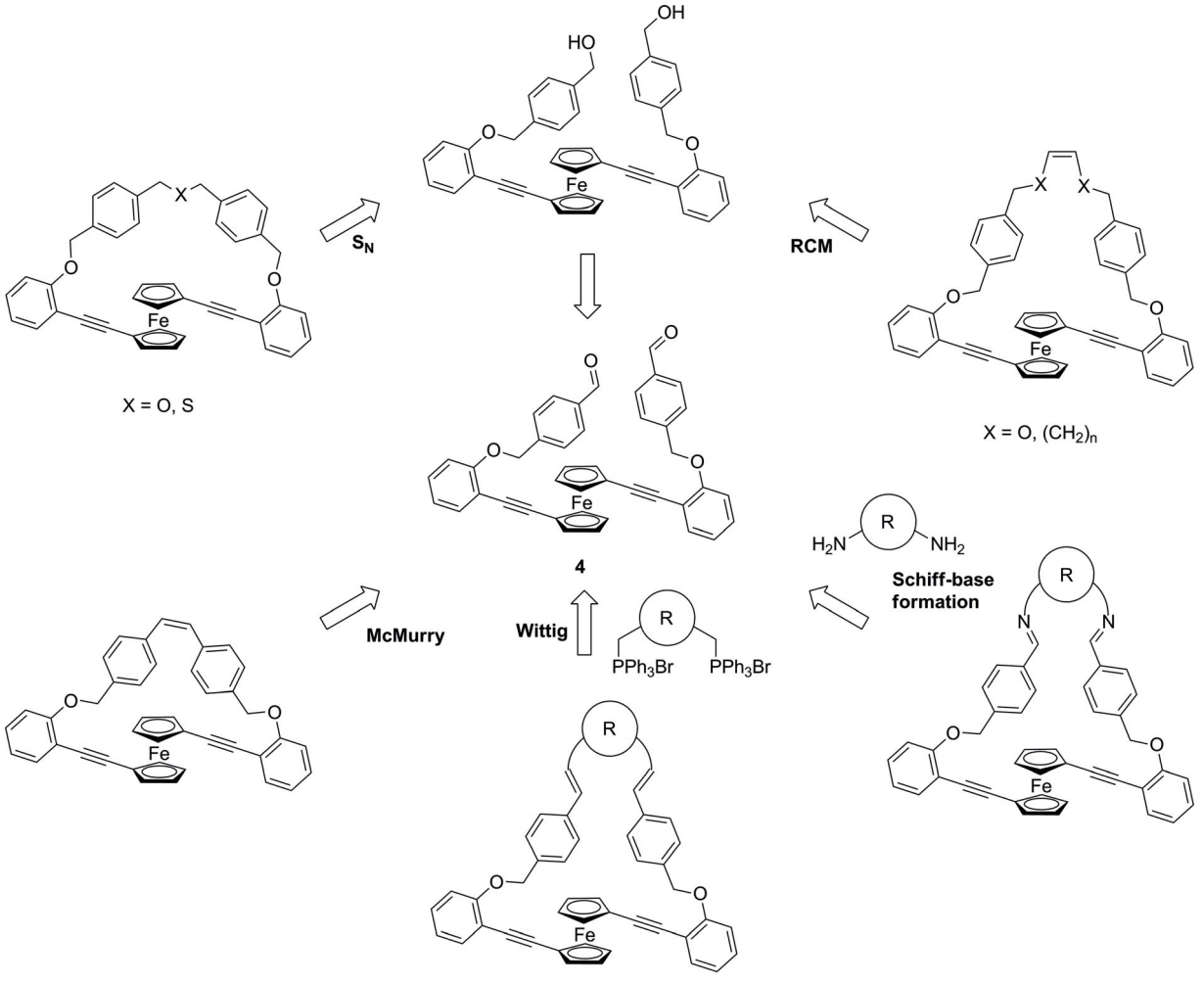

Scheme 2. Different ring-closing strategies with the bis(benzaldehyde) precursor **4** in common.

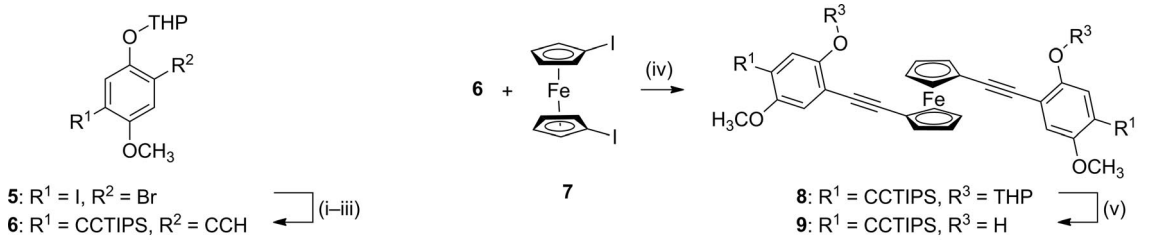

Scheme 3. Synthesis of the molecular rod **9** comprising a central 1,1′-di[(*ortho*-phenol)ethynylene]ferrocene subunit.

selectivity of the iodide group over the bromide group in **5** towards Pd^0-catalyzed cross-coupling conditions.

With the suitably functionalized precursor **9** in hand, numerous attempts to bridge the ferrocene subunit with more- or less-rigid dihalides were performed unsuccessfully. A representative collection of investigated reaction conditions [(i)–(iv)] and dihalides (**10**–**12**) is displayed in Scheme 4. Under all of the investigated nucleophilic reaction conditions, the product formed through the "capping" of the ferrocene junction was not even observed in traces, but 1,1′-di[5-methoxy-6-tris(isopropyl)silylethinylbenzofuran-2-yl]ferrocene (**13**) was detected as the main product instead. This product of a double 5-*endo*-*dig* cyclization clearly shows that the deprotonated phenols prefer to undergo an intramolecular nucleophilic attack at the β-carbon atom of the ethynyl moiety adjacent to the ferrocene, in accordance with Baldwin's rules,[11] instead of the intermolecular reaction with the bridging dihalide. The observed cyclization of 2-ethynyl-substituted phenols to the correspond-

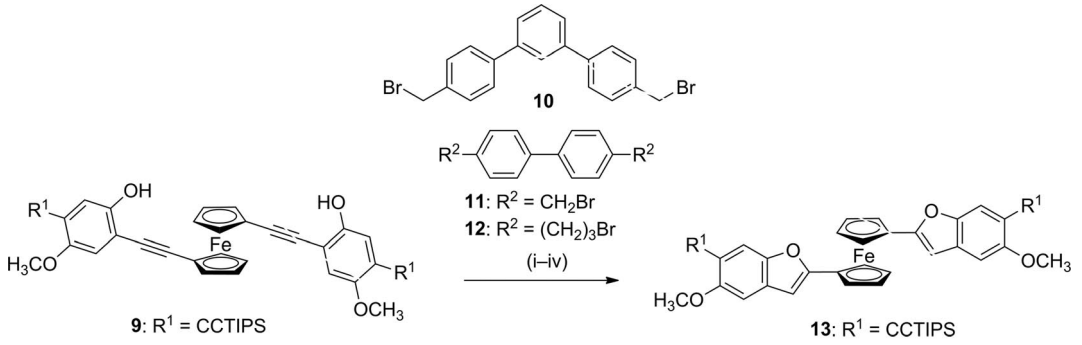

Scheme 4. Unsuccessful capping attempts with the diphenol **9**, which exclusively forms the bis(benzofuran-2-yl)ferrocene derivative **13** under basic reaction conditions; TIPS = triisopropylsilyl.

ing benzofuran derivatives has been proposed as a versatile synthetic route to the heterobicyclic motif[12] and was reported by Babin et al. previously.[13]

As all attempts to form a macrocyclic structure by the capping strategy failed, we refocused our investigation on the bridge-closing strategy. As the capping attempts demonstrated that the phenolate anion at the *ortho* position of the ethynyl group is unacceptable, the bridge-closing strategy has a twofold intrinsic beauty. Not only is the phenol masked but the masking group itself serves as the building block for the assembly of the bridging structure in a later step. As elaborated in the synthetic strategy above, we aimed for a masking group with a benzaldehyde function to provide a promising precursor for a variety of potential macrocyclization reactions. To avoid interference with the assembly of the precursor **4**, the benzaldehyde group was masked as an acetal and introduced as a 1,3-dioxolane motif in **14**.

2-[4(Bromomethyl)phenyl]1,3-dioxolane (**14**) was prepared in two steps according to standard protocols.[14,15] Dioxolane **14** serves as a masked aldehyde and is compatible with the basic cross-coupling conditions shown in Scheme 5. The benzylation of 2-bromophenol (**15**) was performed under basic conditions with K_2CO_3 in *N*,*N*-dimethylformamide (DMF) at 80 °C. The palladium-catalyzed Sonogashira coupling of aryl bromide **16** with a slight excess of 2-methyl-3-butyn-2-ol was performed in a 1:3 mixture of diisopropylamine/tetrahydrofuran (DIPA/THF) with $PdCl_2(PPh_3)_2$ (6 mol-%) and CuI (10 mol-%). The unprotected aldehyde analogue of **16** was also tested but afforded the coupling product in low yields only. The use of 2-methyl-3-butyn-2-ol was preferred over silyl-protected acetylenes, as the polarity introduced by the propargyl alcohol in **17** enabled easy chromatographic purification.[16] The removal of the hydroxypropyl (HOP) group with sodium hydride in toluene under reflux yielded the building block **18** in 72 % yield. Deprotection was also accomplished, yet incomplete, by using a 1 M solution of tetrabutylammonium hydroxide (TBAOH) in methanol at 75 °C by following the Huang protocol.[17]

As 1,1′-diethynyleneferrocene readily undergoes cyclization reactions,[18] **7** was selected as the ferrocene source. Compound **7** was synthesized in two steps by following the protocol of Butler et al.[19] With compound **18** in hand, we were able to perform the twofold Sonogashira coupling reaction shown in Scheme 6. However, this time the reaction conditions developed by Buchwald[20] and co-workers and further optimized for FcI_2 by Inkpen et al.[21] were applied. Thus, $Pd(MeCN)_2Cl_2$/$P(tBu)_3$ with CuI in a DIPA/THF mixture was kept at 60 °C, and a 3:1 ratio of the acetylene **18** was added to FcI_2. The desired symmetrical product **19** was isolated as an orange-red solid in 90 % yield after flash column chromatography (FCC) with silica gel. The subsequent cleavage of the acid-labile dioxolane **19** was accomplished with pyridinium *p*-toluenesulfonate (PPTS) by transacetalization in an acetone/water mixture.[14,22] The deprotection was performed in a sealed microwave tube, and completion was observed after 10 min of irradiation at 80 °C. The reduction of the corresponding aldehyde **4** proceeded in nearly quantitate yields when it was treated with $NaBH_4$ in THF at room temperature for 30 min to form the Fc derivative **20** with two benzylic alcohol groups. Thus, from 2-bromophenol

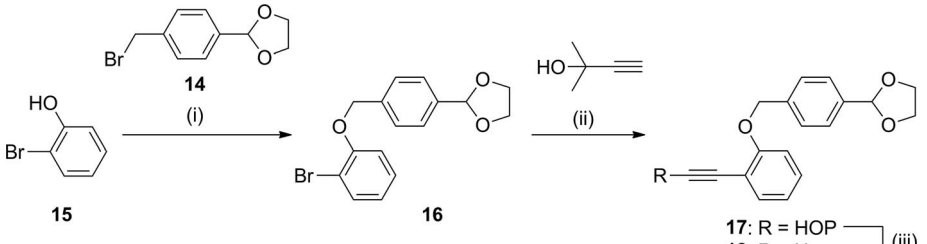

Scheme 5. Synthesis of building block **18**.

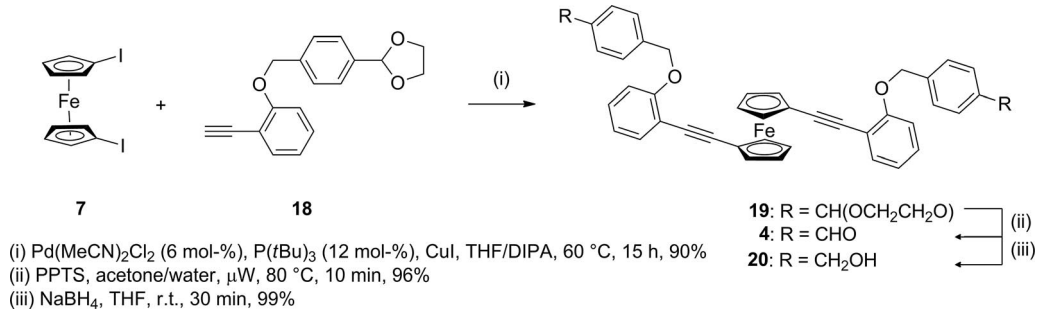

Scheme 6. Sonogashira cross-coupling of FcI_2 and acetylene **18** with subsequent treatment to form the dibenzyl alcohol **20**.

and FcI_2, the molecular rod **20** comprising a ferrocene junction with a benzylic alcohol group on each side was available in six steps and an overall yield of 56 %.

For the bis(benzylic alcohol) **20**, the three different ring-closing strategies displayed in Scheme 7 were investigated. Although an intramolecular S_N2-type reaction was considered in the first approach (route a), the macrocyclizations in the second and third approaches were based on the ring-closing metathesis reactions of terminal olefins. In the second strategy (route b), olefins were introduced with a Grignard reagent, and terminal olefins were introduced by ether formation in the third attempt (route c). In route a (Scheme 7), one of the two benzylic alcohols of **20** should be converted into a good leaving group to enable the intramolecular attack by the other one. Therefore, an oven-dried Schlenk flask was purged with argon and charged with a 4.5 mM solution of diol **20** in dry and deoxygenated THF. The reaction mixture was cooled to –10 °C and treated with sodium hydride. The mixture was stirred for 20 min, and then methanesulfonyl chloride (2.0 equiv.) was added. The reaction was allowed to reach room temperature over 16 h. The elongated reaction times at room temperature resulted in the substantial decomposition of the mesylate intermediates, as depicted in Figure S1 (Supporting Information). The gentle heating of the mesylate reaction mixture to 50 °C results in the formation of macrocycles of varying ring size, as shown in Figure S2. Hence, we decided to convert the mesylate intermediates into the bromo analogs through the addition of lithium bromide to the reaction mixture.[23] The products **21** and **22** were separated from the remaining starting material by silica gel flash column chromatography in 33 and 40 % yield, respectively. A 0.5 mM suspension of monobromo **21** and an excess of sodium hydride in dry THF gave the desired ether-bridged macrocycle **1** in an excellent 70 % yield after 2 h at 70 °C (see Figure S3). Furthermore, efforts to trigger the ether-

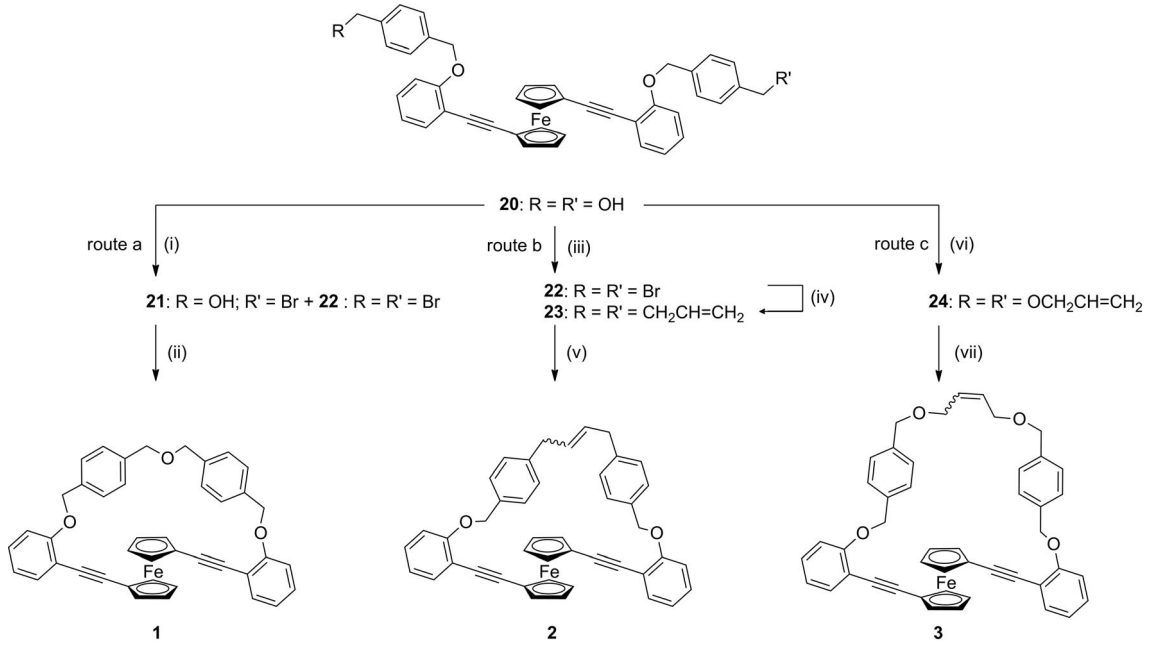

Scheme 7. Ring-closing reactions to form the proposed dibenzylic bridges of different lengths.

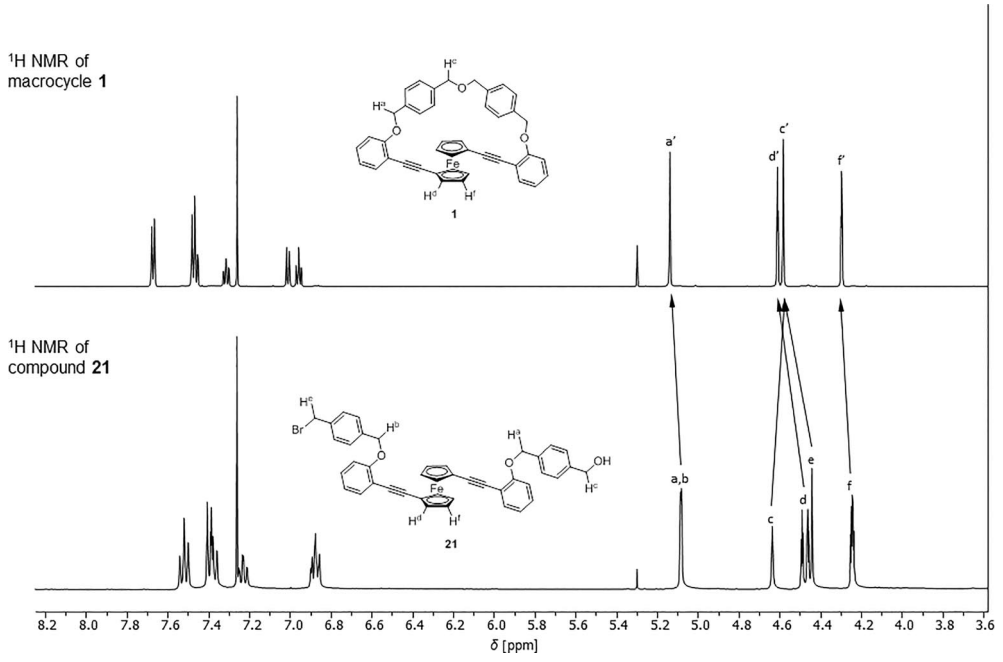

Figure 2. ^{1}H NMR spectra of **1** and **21** in $CDCl_3$ at 20 °C.

bridge formation through the activation of one benzylic alcohol in an intramolecular Mitsunobu-type reaction failed. The successful macrocyclization was indicated by the mass of the isolated compound recorded by MALDI-TOF MS (Figure S14) and further corroborated by ^{1}H NMR spectroscopy. As depicted in Figure 2, compound **21** nicely shows two separate signals for its methylene protons at δ = 4.63 (s, 2 H, H^c geminal to OH) and 4.44 ppm (s, 2 H, H^e next to Br), whereas they merge into a common benzyl ether signal for symmetric compound **1** at δ = 4.58 ppm (s, 4 H, H^c) as indicated with an arrow. The benzylic protons H^a and H^b in **21** produce two overlapping singlets and likewise culminate as H^a in macrocycle **1**. More profoundly, the ferrocene protons of open-structure **21** are seen as four pseudotriplets with α-protons H^d at δ = 4.49 (pseudo-t, J = 1.9 Hz, 2 H) and 4.46 ppm (pseudo-t, J = 1.9 Hz, 2 H) as well as two upfield-shifted and overlapping β-protons H^f as pseudotriplets at δ = 4.25 (pseudo-t, J = 1.9 Hz, 2 H) and 4.24 ppm (pseudo-t, J = 1.9 Hz, 2 H). This splitting can be explained by the magnetic inequivalence of the two α-protons and the two β-protons of each Cp ring. Hence, the ferrocene protons of **21** are seen as two high-order AA′MM′ and BB′XX′ spin systems with four signals in total. In contrast, the spectrum of fully symmetric macrocycle **1** shows only two pseudotriplets at δ = 4.61 (pseudo-t, J = 1.8 Hz, 4 H, H^d) and 4.30 ppm (pseudo-t, J = 1.8 Hz, 4 H, H^f) as one AA′MM′ high-order spin system.

To obtain a heteroatom-free bridging structure, we focused on RCM as a potential ring-closing route (Scheme 7, routes b and c). As a promising precursor, we identified the ferrocene rod **23** with two (4-allylbenzyl)oxy substituents. Thus, diol **20** was converted into the dimesylate derivative (Scheme 7, route b) by the treatment of the benzylic alcohol with an excess of sodium hydride at –10 °C and the subsequent addition of 10 equiv. of methanesulfonyl chloride in dry and deoxygenated THF. After the reaction warmed to room temperature, full conversion was indicated by MALDI-TOF MS after 16 h (see Figure S3). The subsequent addition of 20 equiv. of LiBr in an argon atmosphere reliably gave the dibromo derivative **22** after 2 h at room temperature. The product was isolated in 69 % yield after purification through a short silica gel column as a red oil that crystalized upon standing. Then, dibromo compound **22** was treated with 20 equiv. of a 1 M solution of vinylmagnesium bromide in THF in the presence of CuI (1.0 equiv.) at –70 °C.[24] The reaction mixture was warmed to room temperature over 15 h, and mass spectrometry showed the full consumption of the starting material. After aqueous workup and extraction, the crude product was purified by FCC with silica gel, and diallylbenzyl **23** was isolated as a red-orange oil in 67 % yield. The analysis of the isolated side products by mass spectrometry (MALDI-TOF MS spectra in Figure S4) indicated the formation of an ethane-bridged macrocycle together with di- and trimeric open structures; this suggests that dibromobenzyl **22** undergoes intra- and intermolecular Grignard reactions under these reaction conditions. With the diolefin in hand, we were able to investigate the RCM reaction. Therefore, a 1.0 mM solution of divinyl **23** in freshly distilled dichloroethane was prepared and heated together with 15 mol-% of the first-generation Grubbs catalyst for 16 h at 70 °C. Macrocycle **2** was isolated in 57 % yield as an inseparable mixture of *E* and *Z* isomers after column chromatography. The formation of an *E*/*Z* mixture was not surprising as we did not use an *E*- or *Z*-selective RCM catalyst nor does our compound bear structural determinants. However, the macrocycle was evidenced by mass spectrometry analysis and we also identified the configuration of the target compound (*E*/*Z*)-**2** by one- and two-dimensional NMR spectroscopy experiments (Figure S17). The unambiguous determination of the *E* and *Z* isomers is hampered by the symmetry of the two stereoisomeric compounds. The two vinyl protons $H^{aE/Z}$ in (*E*/*Z*)-**2** are symmetry-equivalent and isochronous in both cases, and the

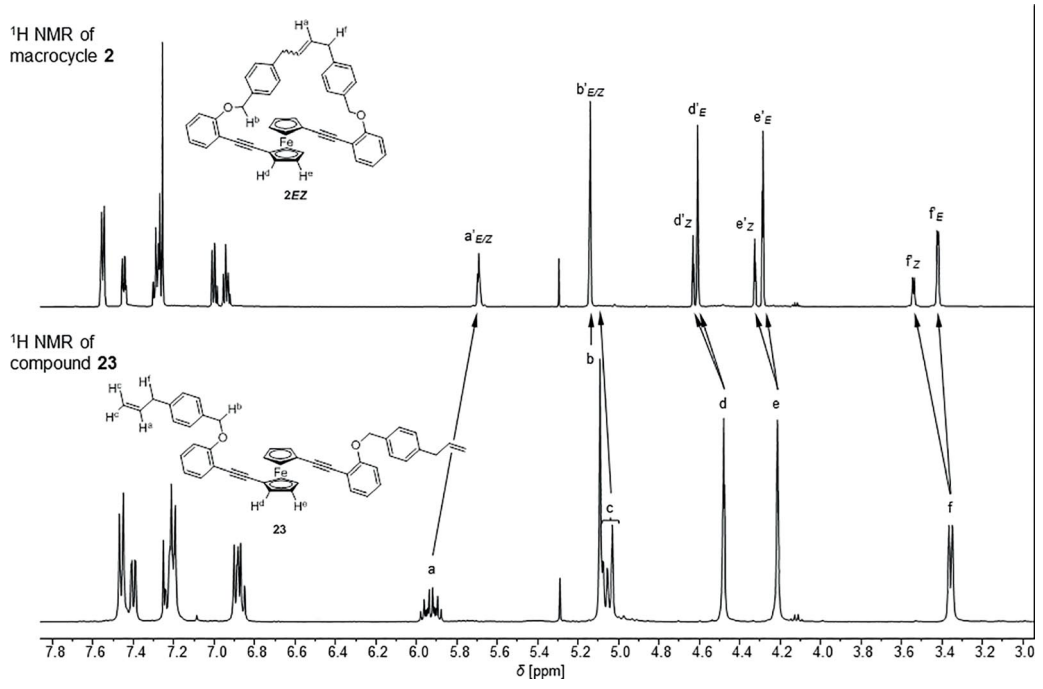

Figure 3. ^{1}H NMR spectra of **2** and **23** in $CDCl_3$ at 20 °C.

coupling to the two adjacent methylene groups results in magnetically inequivalent protons, which show high-order spectra that cannot be analyzed directly. Consequently, we recorded a 2D heteronuclear single quantum coherence (HSQC) spectrum that showed a chemical-shift difference of 5.3 ppm along the carbon dimension; this allows the unambiguous assignment of the major species as the *E* isomer with δ = 38.7 ppm, whereas the minor *Z* isomer resonates at δ = 33.4 ppm (Figure S17). The ^{1}H NMR spectra of macrocycle **2** and its precursor **23** are shown in Figure 3. The characteristic signal of the vinylic methine proton H^a in **23** merges from δ = 5.93 ppm (ddt, *J* = 16.9 Hz, 10.2 Hz, 6.7 Hz, 2 H) to an overlapping signal for both isomers at δ = 5.69 ppm (m, 2 H, $H^{aE/Z}$). The signals of the allylic protons H^f in **23** diverge for the *E* and *Z* isomer into doublets at δ = 3.54 (d, *J* = 5.1 Hz, 2 H, H^{fZ}) and 3.42 ppm (d, *J* = 4.9 Hz, 2 H, H^{fE}). The signals of the terminal olefin protons H^c in **23** completely disappear in the spectrum of the macrocycle. The structural changes affect the benzylic protons H^b slightly, as the change is only $\Delta\delta$ = 0.047 ppm. Finally, the ferrocene signals draw a coherent picture of the formed macrocycle. We observed the ferrocene protons at δ = 4.63 (pseudo-t, *J* = 1.8 Hz, 4 H, H^{dZ}), 4.33 (pseudo-t, *J* = 1.8 Hz, 4 H, H^{eZ}), 4.61 (pseudo-t, *J* = 1.8 Hz, 4 H, H^{dE}), and 4.29 ppm (pseudo-t, *J* = 1.8 Hz, 4 H, H^{eE}), in accordance with the above-stated splitting system for symmetrically substituted ferrocenes. The *E*/*Z* ratio was calculated by comparing the integrals for the allylic protons H^{fE} and H^{fZ} and was found to be 2.8:1.

To further elongate the bridging unit, we planned to connect the benzyl moieties through an allyl ether bridge (Scheme 7, route c). The diol **20** was treated in a dry and deoxygenated THF solution with sodium hydride (4.0 equiv.) at room temperature, followed by the addition of allyl bromide (4.0 equiv.) and heating at 60 °C for 5 h. The product **24** was isolated by silica gel column chromatography as an orange solid in 60 % yield. For the final ring-closing reaction, diallyl ether **24** was kept at 60 °C in a 1.3 mM solution of dichloroethane and 7.5 mol-% of the first-generation Grubbs catalyst. Full conversion was observed after 20 h, and macrocycle **3** was isolated in 57 % yield as a mixture of *E* and *Z* isomers after silica gel column chromatography. The mixture was separated through semipreparative HPLC to give 73 % of the *E* isomer and 27 % of the *Z* isomer. We identified the two isomers by recording a double-quantum-filtered, carbon-coupled 1D HMQC-type spectrum, in which only the protons bound to ^{13}C nuclei give a detectable signal. The differences in the ^{1}H–^{1}H coupling constants clearly allow the assignment of the *Z* ($^3J_{H,H}$ = 11.5 Hz) and *E* isomers ($^3J_{H,H}$ = 15.8 Hz), as shown in Figure S19. Further, the ^{13}C chemical-shift difference for the adjacent CH_2 group additionally validates these findings (*E* at δ = 69.9 ppm and *Z* at δ = 65.0 ppm), as they display the well-known gamma effect.[25] In Figure 4, we pinpoint the structural changes with the help of ^{1}H NMR spectroscopy. The signal of the vinylic methine protons H^a in **24** at δ = 5.93 ppm (ddt, *J* = 17.2 Hz, 10.4 Hz, 5.6 Hz, 2 H) diverges into H^{aE} at δ = 5.88 ppm (m, 2 H) in (*E*)-**3** and H^{aZ} at δ = 5.78 ppm (m, 2 H) in (*Z*)-**3**. The signals of the olefin protons H^b and H^c in **24** disappeared in the spectra of the *E* and *Z* isomers of the macrocycle **3**. The signals of the benzylic protons H^d are both slightly high-field-shifted in the spectra of the macrocycles, whereas those of the methylene protons H^f showed an inverse trend for the *E* and *Z* isomer, as the signal of H^{fE} at δ = 5.09 ppm (s, 4 H) is shifted slightly downfield, and that of H^{fZ} at δ = 4.43 ppm (s, 4 H) shifts upfield. More connotative is the strong downfield shift for the ferrocene α-protons from the open structure in **24** to the closed macrocycles; $\Delta\delta$ = 0.31 ppm for $H^{g'E}$ in (*E*)-**3**, and $\Delta\delta$ = 0.26 ppm for H^{gZ} in (*Z*)-**3**. Less explicit is the change in the ferrocene β-protons; $\Delta\delta$ = 0.22 ppm for

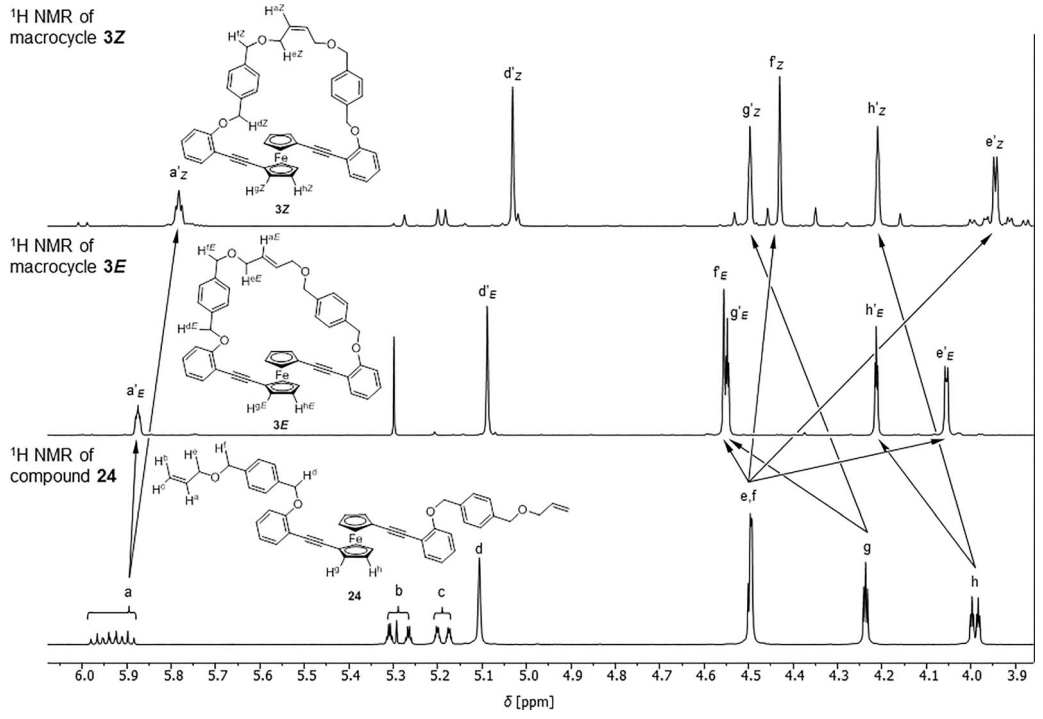

Figure 4. ^{1}H NMR spectra of (*E*)-**3**, (*Z*)-**3**, and **24** in $CDCl_3$ at 20 °C.

H^{hE} in (*E*)-**3**, and $\Delta\delta$ = 0.22 ppm for H^{hZ} in (*Z*)-**3**. We attribute this variation to local magnetic anisotropic effects, which arise from "edge-pointing" aromatic bridging rings that are forced into the ferrocene space. On the other hand, the allylic protons H^e in **24** are strongly deshielded, whereas the protons $H^{e'E}$ and $H^{e'Z}$ in the macrocyclic compounds are twisted out of the olefinic plane and their ^{1}H NMR signals are shifted strongly upfield, as depicted in Figure 4.

Numerous attempts to grow single crystals of macrocycles **1**–**3** failed, and we initially attributed this to the high flexibility of the bridging structure. This hypothesis was incorrect, as single crystals suitable for X-ray diffraction analysis were obtained of the macrocycle (*Z*)-**3**, which has a particularly long and flexible bridging structure, by solvent-diffusion crystallization in a dichloromethane/2-propanol (DCM/2-propanol) system. The solid-state structure is displayed in Figure 5 and corroborated both the identity of (*Z*)-**3** and our assignment of the structures from the NMR spectra. Although the structural affirmation is pleasing, the solid-state structure challenges our molecular design. Clearly, the bridging structure is too flexible to enforce a stretched arrangement of the phenyl–ethynyl–Fc–ethynyl–phenyl substructure, at least in the solid state. Instead, (*Z*)-**3** crystallizes in a hook-shaped arrangement with nearly parallel phenylethynyl moieties and a dihedral angle of 9.95° enclosed by both ethynyl groups. The interplanar distance of 3.723 Å measured between both centers of the phenyl rings (d_1 in Figure 5) suggests considerable π–π interactions between the phenylethynyl subunits. Owing to this stacked confirmation, the *Z*-allyl ether bridge forms a loop that is tilted to one side of the macrocycle and causes the distance between O_1 and O_4 to be only 3.551 Å (d_2 in Figure 5). Another eye-catching structural feature is the proximity of the ferrocene hydrogen atoms and the phenyl rings of the bridging linker. The ferrocene α- and β-hydrogen atoms next to the linking loop are both located at the periphery of the phenyl rings, in agreement with the strong downfield proton shift observed for the ferrocene α- and β-protons upon the formation of (*Z*)-**3** and (*E*)-**3** (Figure 4). The hook-shaped arrangement of (*Z*)-**3** is mainly present in the solid-state structure owing to crystal-packing forces, and the dissolved molecule must have a structural flexibility that results in single signals for the ferrocene α- and β-protons in the ^{1}H NMR spectrum (Figure 4). Attempts to freeze out the molecular motion were unsuccessful, as the ^{1}H NMR spectrum of (*Z*)-**3** at –80 °C in CD_2Cl_2 still displayed a single signal for all four ferrocene α-protons. The averaging flexibility of the dissolved molecule must also comprise rotational motion around the ferrocene axis.

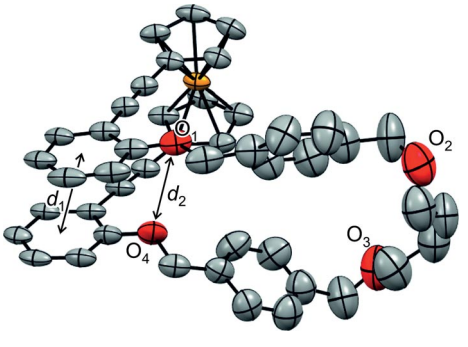

Figure 5. ORTEP plot of the solid-state structure of (*Z*)-**3** with ellipsoids plotted at the 50 % probability level.

Notably, only the 1H NMR spectra of macrocycles (*Z*)-**3** and (*E*)-**3** display a pronounced downfield shift for the ferrocene protons; this points to a somewhat coplanar arrangement of the phenyl rings in the bridging structure and the cyclopentadienyl rings of the ferrocene subunit. For the cyclizations to macrocycles **1**, (*E*)-**2**, and (*Z*)-**2**, only a slight effect on the chemical shift of the ferrocene α- and β-protons was observed (Figures 2 and 3). This does not exclude a rotation of the ferrocene joint but implies that the bridge rings are at least less frequently located in plane with the cyclopentadienyl rings in solution.

Conclusions

In this paper, a short and convergent access to rotationally restricted 1,1′-disubstituted ferrocene diphenylethynyl macrocycles is reported. A bridge-closing strategy enabled the formation of the five macrocyclic structures **1**, (*E*)-**2**, (*Z*)-**2**, (*E*)-**3**, and (*Z*)-**3** with various ring sizes, which were obtained either by ring-closing metathesis or by an intramolecular nucleophilic substitution reaction. The macrocyclization provided these structures in reasonable yields of 57–70 %, and the mixtures of *E* and *Z* olefins obtained by the metathesis reactions could only be separated for (*E*)-**3** and (*Z*)-**3**. However, the composition of the reaction mixture for (*E*)-**2** and (*Z*)-**2** was analyzed by assignment and integration of the signals in the NMR spectra.

Although the integration of the 1,1′-di(phenylene-ethynylene)ferrocene subunit into a macrocycle restricts the rotation of the ferrocene axis, the intended fixation of a stretched arrangement of the 1,1′-di(phenylene-ethynylene)ferrocene junction could not be realized with the presented macrocycles. The solid-state structural of (*Z*)-**3** instead displayed a stacked arrangement of the two phenylethynyl subunits. These macrocyclic structures display a dynamic behavior in solution, and the large variety of angles between both Fc-interlinked phenylethynyl subunits clearly shows that these bridging structures are too flexible to favor a particular arrangement of the Fc junction in solution.

However, the benzaldehyde-functionalized precursor provides access to a variety of alternative bridge-closing reactions, and our current focus is set on bridging subunits with increased stiffness.

Experimental Section

General Information: All commercially available compounds were purchased from Sigma–Aldrich, Acros, Apollo Scientific, Alfa Aesar, and Fluorochem and used as purchased. Dry solvents were purchased from Sigma–Aldrich and Acros and stored over molecular sieves (4 Å). $PdCl_2(MeCN)_2$ was synthesized by heating $PdCl_2$ in acetonitrile under reflux for 1 h. The resulting solution was filtered through Celite and concentrated to crystallize the product, which was washed with acetonitrile and diethyl ether and then dried in air.[21] THF and DCM were distilled from CaH_2 for 6 h in an argon atmosphere. DIPA was distilled and stored over activated molecular sieves (4 Å). The reaction flasks used for acetylene deprotection were washed successively with concentrated sulfuric acid, aq. 1 M NaOH solution, and deionized water and then dried under vacuum before use. HPLC purification was achieved with a Shimadzu LC-20 AB system, a Reprosil 100 Å Si, 5 µm, 250 × 16 mm column from Dr. Maisch, HPLC-grade 2-propanol from Biosolve, and hexane form Baker. For column chromatography, silica gel P60 (40–63 µm) from Silicycle™ was usually used, and the solvents were of technical grade. TLC was performed with silica gel 60 F254 glass plates with a thickness of 0.25 mm purchased from Merck. All 2D NMR spectra were recorded with a Bruker Ascend 600 MHz Avance III HD spectrometer equipped with a 5 mm QCI cryogenic probehead. The ^1H and ^{13}C NMR spectra were recorded with a Bruker DPX NMR spectrometer at 400 and 101 MHz or a Bruker BZH NMR spectrometer at 250 and 63 MHz. The chemical shifts are reported in ppm relative to tetramethylsilane or referenced to a residual solvent peak, and the *J* values are given in Hz (±0.1 Hz). High-resolution mass spectra (HRMS) were measured with a Bruker Maxis 4G ESI-TOF instrument or a Bruker solariX spectrometer with a MALDI source. The MALDI-TOF mass spectra were recorded with a Bruker Microflex LRF spectrometer and were calibrated by using CsI_3 clusters.[26] *trans*-2-[3-(4-*tert*-Butylphenyl)-2-methyl-2-propenylidene]-malononitrile (DCTB) was used as the matrix if needed.[27] GC–MS was performed with a Shimadzu GC-MS-2020 SE instrument equipped with a Zebron 5 MS Inferno column, which allowed temperatures of up to 350 °C. Elemental analyses were performed with an Elementar Vario Micro Cube instrument.

2-[4-(Bromomethyl)phenyl]-1,3-dioxolane (14): This compound was synthesized in two steps by adapting related protocols.[14,15] An oven-dried two-necked round-bottomed flask was purged with argon and charged with 4-(bromomethyl)benzonitrile (5.00 g, 24.2 mmol), which was dissolved in dry dichloromethane (100 mL). The solution was cooled to −70 °C, and then a solution of DIBAL-H (1 M in hexane, 26.7 mL, 26.7 mmol) was added with a dropping funnel. After the addition, the mixture was warmed to 0 °C over 1 h. Then, the mixture was slowly quenched by the addition of aqueous 1 M HCl solution (10 mL) and warmed to room temperature. The mixture was eluted with toluene (250 mL) and washed sequentially with aqueous 1 M HCl solution, 1 M NaOH solution, water (2 ×), and brine. The organic phase was separated, dried with $MgSO_4$, filtered, and concentrated under reduced pressure. The crude product was purified by silica FCC with EtOAc/cyclohexane (1:5) as the eluent. Upon the evaporation of the solvent, 4-(bromomethyl)benzaldehyde was obtained as an off-white solid, yield 84 % (4220 mg, 21.3 mmol). ^1H NMR (400 MHz, $CDCl_3$, 25°C): δ = 10.01 (s, 1 H), 7.93–7.81 (m, 2 H), 7.61–7.50 (m, 2 H), 4.51 (s, 2 H) ppm. ^{13}C NMR (101 MHz, $CDCl_3$, 25°C): δ = 191.47, 144.24, 136.14, 130.16, 129.66, 31.94 ppm. MS (EI+, 70 eV): *m/z* (%) = 198 (4), 119 (100), 91 (75), 63 (20). C_8H_7BrO (197.97): calcd. C 48.27, H 3.54; found C 48.25, H 3.81.

A round-bottomed flask was charged with 4-(bromomethyl)benzaldehyde (4.10 g, 22.9 mmol), which was dissolved in toluene (80 mL). To the solution, ethylene glycol (2.55 mL, 45.7 mmol) and a catalytic amount of *p*-toluenesulfonic acid (10 mol-%) were added, and the mixture was heated under reflux with the aid of a Dean–Stark trap for 12 h. After no more water was segregated, the reaction was stopped and eluted with toluene (100 mL). Then, the mixture was washed with water (2 × 150 mL) and brine. The organic phase was separated, dried with $MgSO_4$, filtered, and concentrated under reduced pressure. The product was purified by silica FCC with EtOAc/cyclohexane (1:5) as the eluent. Upon the evaporation of the solvent, **14** was obtained as a colorless liquid, which solidified upon standing. Data for **14**: Yield 91 % (5040 mg, 20.8 mmol). ^1H NMR (400 MHz, $CDCl_3$, 25°C): δ = 7.48–7.44 (m, 2 H), 7.43–7.38 (m, 2 H), 5.81 (s, 1 H), 4.49 (s, 2 H), 4.17–3.98 (m, 4 H) ppm. ^{13}C NMR (63 MHz,

$CDCl_3$, 25°C): δ = 138.77, 138.34, 129.16, 126.99, 103.34, 65.41, 33.12 ppm. MS (EI+, 70 eV): *m/z* (%) = 241 (9), 163 (100), 91 (70), 73 (23). $C_{10}H_{11}BrO_2$ (241.99): calcd. C 49.41, H 4.56; found C 49.31, H 4.28, N 0.4.

2-{4-[(2-Bromophenoxy)methyl]phenyl}-1,3-dioxolane (16): A round-bottomed flask was charged with 2-bromophenol (581 mg, 3.29 mmol), which was then dissolved in dry DMF (20 mL). To that solution, 2-[4-(bromomethyl)phenyl]-1,3-dioxolane (800 mg, 3.29 mmol) and potassium carbonate (919 mg, 6.58 mmol) were added. The mixture was stirred overnight at 80 °C. After the reaction was completed, the reaction mixture was poured onto a saturated solution of aqueous NH_4Cl (100 mL). The aqueous phase was extracted with three portions of toluene (50 mL). The organic phases were combined and washed with water (2 × 100 mL) and brine, dried with $MgSO_4$, and filtered, and the volatiles were removed under reduced pressure. The crude product was purified by silica gel FCC with EtOAc/cyclohexane (1:5) as the eluent. Upon the evaporation of the volatiles, the title compound was isolated as an off-white solid, yield 94 % (1050 mg, 3.14 mmol). ^{1}H NMR (400 MHz, $CDCl_3$, 25°C): δ = 7.56 (dd, $^3J_{H,H}$ = 7.9, $^4J_{H,H}$ = 1.6 Hz, 1 H), 7.53–7.47 (m, 4 H), 6.91 (dd, $^3J_{H,H}$ = 8.3, $^4J_{H,H}$ = 1.4 Hz, 1 H), 6.84 (dd, $^3J_{H,H}$ = 7.9, $^4J_{H,H}$ = 1.4 Hz, 1 H), 5.83 (s, 1 H), 5.18 (s, 2 H), 4.19–3.96 (m, 4 H) ppm. ^{13}C NMR (63 MHz, $CDCl_3$, 25°C): δ = 155.07, 137.80, 137.75, 133.59, 128.53, 127.11, 126.88, 122.34, 114.04, 112.64, 103.65, 70.61, 65.47 ppm. MS (EI+, 70 eV): *m/z* (%) = 334 (1.5), 163 (67), 119 (15), 91 (100). $C_{16}H_{15}BrO_3$ (335.02): calcd. C 57.33, H 4.51; found C 57.07, H 4.63.

4-(2-{[4-(1,3-Dioxolan-2-yl)benzyl]oxy}phenyl)-2-methylbut-3-yn-2-ol (17): An oven-dried 25 mL Schlenk tube was purged with argon and charged under a positive pressure of argon with CuI (136 mg, 0.712 mmol, 10 mol-%), $Pd(PPh_3)_2Cl_2$ (303 mg, 0.427 mmol, 6 mol-%), and aryl bromide **16** (2.72 g, 7.12 mmol). The mixture was suspended in a previously deoxygenated mixture of THF and diisopropylamine (15 mL, 3:1). Then, 2-methyl-3-butyn-2-ol (3.55 mL, 35.6 mmol) was added dropwise with a syringe, and the reaction was heated to 80 °C for 15 h. After the reaction was completed, the mixture was suspended on Celite and eluted with DCM. The volatiles were removed, and the dry powder was subjected to silica gel FCC with EtOAc/cyclohexane (1:3 to 1:1). The solvent was removed under reduced pressure to afford the title compound as a colorless oil, yield 70 % (1650 mg, 4.98 mmol). ^{1}H NMR (400 MHz, $CDCl_3$, 25°C): δ = 7.51–7.43 (m, 4 H), 7.37 (dd, $^3J_{H,H}$ = 7.5, $^4J_{H,H}$ = 1.7 Hz, 1 H), 7.20 (td, $^3J_{H,H}$ = 7.7, $^4J_{H,H}$ = 1.5 Hz, 1 H), 6.88 (d, $^3J_{H,H}$ = 7.5 Hz, 1 H), 6.84 (d, $^3J_{H,H}$ = 8.5 Hz, 1 H), 5.79 (s, 1 H), 5.09 (s, 2 H), 4.14–3.94 (m, 4 H), 2.83 (s, 1 H), 1.60 (s, 6 H) ppm. ^{13}C NMR (63 MHz, $CDCl_3$, 25°C): δ = 159.10, 138.10, 137.36, 133.38, 129.59, 126.70, 126.64, 120.91, 112.90, 112.74, 103.51, 98.46, 78.33, 77.21, 69.94, 65.58, 65.28, 31.56, 31.06 ppm. HRMS (ESI-TOF): calcd. for $C_{21}H_{22}O_4Na$ $[M + Na]^+$ 361.1410; found 361.1418.

2-{4-[(2-Ethynylphenoxy)methyl]phenyl}-1,3-dioxolane (18): An oven-dried 50 mL round-bottomed flask was equipped with a reflux condenser, purged with argon, and charged with **17** (1171 mg, 3.46 mmol), which was then dissolved in previously deoxygenated dry toluene (30 mL). Then, NaH (60 % dispersion in mineral oil, 85.2 mg, 2.13 mmol) was added in one portion, and the resulting mixture was heated to reflux overnight (12 h). After the reaction was completed, the mixture was eluted with toluene (50 mL) and washed with water (2 × 100 mL) and brine. The organic phase was dried with $MgSO_4$ and filtered, and the volatiles were removed under reduced pressure. The crude product was purified by silica gel column chromatography with EtOAc/cyclohexane (1:5) as the eluent. Upon the evaporation of the volatiles, the title compound was isolated as a pale yellow oil, yield 72 % (694 mg, 2.48 mmol) ^{1}H NMR (400 MHz, $CDCl_3$, 25°C): δ = 7.52–7.46 (m, 5 H), 7.28–7.21 (m, 1 H), 6.91 (td, $^3J_{H,H}$ = 7.5, $^4J_{H,H}$ = 1.0 Hz, 1 H), 6.89–6.85 (m, 1 H), 5.82 (s, 1 H), 5.20 (s, 2 H), 4.20–3.98 (m, 4 H), 3.31 (s, 1 H) ppm. ^{13}C NMR (63 MHz, $CDCl_3$, 25°C): δ = 159.65, 137.92, 137.48, 134.17, 130.11, 126.86, 126.71, 120.82, 112.70, 112.04, 103.54, 81.36, 80.03, 70.09, 65.33 ppm. MS (EI+, 70 eV): *m/z* (%) = 279 (6), 208 (11), 163 (36), 91 (100). $C_{18}H_{16}O_3$ (280.11): calcd. C 77.12, H 5.75; found C 77.35, H 5.87.

Compound 19: An oven-dried 15 mL Schlenk tube was purged with argon and charged with $Pd(MeCN)_2Cl_2$ (12.9 mg, 0.049 mmol, 6 mol-%), copper iodide (15.7 mg, 0.08 mmol, 10 mol-%), and 1,1′-diiodoferrocene (359 mg, 0.82 mmol) under a positive pressure of argon. Then, freshly distilled and deoxygenated THF (9 mL) was added together with the ligand P(*t*Bu)$_3$ (24.8 µL, 0.09 mmol, 12 mol-%). Phenylacetylene **18** (690 mg, 2.46 mmol) was dissolved in freshly distilled and deoxygenated DIPA (3 mL) and added to the reaction mixture. The oil bath was heated to 60 °C, and the mixture was stirred overnight (20 h). The black reaction mixture was suspended on Celite and eluted with DCM. The volatiles were removed, and the dry powder was subjected to silica gel FCC with EtOAc/cyclohexane (1:5) as the eluent to isolate the mono- and disubstituted ferrocene derivative **19** as a red oil, yield 90 % (550 mg, 0.74 mmol). ^{1}H NMR (400 MHz, $CDCl_3$, 25°C): δ = 7.59–7.47 (m, 8 H), 7.41–7.37 (m, 2 H), 7.23–7.17 (m, 2 H), 6.89–6.83 (m, 4 H), 5.81 (s, 2 H), 4.52 (pseudo-t, $^3J_{H,H}$ = 1.9 Hz, 4 H), 4.26 (pseudo-t, $^3J_{H,H}$ = 1.9 Hz, 4 H), 4.10–3.98 (m, 8 H) ppm. ^{13}C NMR (63 MHz, $CDCl_3$, 25°C): δ = 158.98, 138.16, 137.50, 133.16, 128.92, 126.94, 126.60, 120.85, 113.98, 112.65, 103.50, 91.71, 82.63, 72.86, 71.33, 70.00, 67.03, 65.25 ppm. HRMS (MALDI/ESI): calcd. for $C_{46}H_{38}FeO_6$ $[M]^+$ 742.2013; found 742.2013.

Compound 4: A 20 mL oven-dried argon-flushed microwave vial was charged with **19** (163 mg, 0.219 mmol), pyridinium *p*-toluenesulfonate (226 mg, 0.262 mmol), and a solvent mixture of absolute acetone (12.75 mL) and water (2.25 mL). The microwave vial was sealed and heated in a microwave oven for 10 min at 80 °C. After the vial cooled to room temperature, the solvent was removed in vacuo, and the remaining substance was dissolved in *tert*-butyl methyl ether (*t*BME, 80 mL) and washed with aqueous $NaHCO_3$ (2 × 50 mL), water, and brine. The organic phase was dried with $MgSO_4$ and concentrated in vacuo to afford the title compound as a red solid, yield 87 % (125 mg, 0.190 mmol). ^{1}H NMR (400 MHz, $CDCl_3$, 25 °C): δ = 9.90 (s, 2 H), 7.84 (d, $^3J_{H,H}$ = 8.1 Hz, 4 H), 7.67 (d, $^3J_{H,H}$ = 7.8 Hz, 4 H), 7.38–7.34 (m, 2 H), 7.22–7.16 (m, 2 H), 6.88–6.82 (m, 2 H), 6.78–6.73 (m, 2 H), 5.01 (s, 4 H), 4.57–5.50 (m, 4 H), 4.36–4.31 (m, 4 H) ppm. ^{13}C NMR (63 MHz, $CDCl_3$, 25°C): δ = 191.90, 158.52, 144.06, 135.76, 133.07, 129.87, 129.00, 126.98, 121.17, 113.97, 112.32, 91.78, 82.93, 73.00, 70.96, 69.23, 67.50 ppm. HRMS (MALDI/ESI): calcd. for $C_{42}H_{30}FeO_4$ $[M]^+$ 654.1489; found 654.1489.

Compound 20: An oven-dried, argon-flushed 50 mL round-bottomed flask was charged with **4** (0.191 mol, 125 mg), which was then dissolved in dry THF (20 mL). To the clear bright orange solution, $NaBH_4$ (30 mg) was added in one portion. The reaction was stirred for 45 min at room temperature, after which TLC showed full conversion. The reaction mixture was cooled to 0 °C, and aq. NH_4Cl (20 %, 20 mL) was added slowly. After extraction with *t*BME, the combined organic phases were washed with water and brine and dried with anhydrous $MgSO_4$, and the solvent was removed in vacuo. The residue was purified by silica gel FCC with EtOAc/cyclohexane (1:1) as the eluent to isolate **20** as a bright red-orange solid. ^{1}H NMR (400 MHz, $CDCl_3$, 25°C): δ = 7.52 (d, $^3J_{H,H}$ = 7.7 Hz, 3 H), 7.39 (dd, $^3J_{H,H}$ = 7.8, $^4J_{H,H}$ = 1.7 Hz, 2 H), 7.35 (d, $^3J_{H,H}$ = 7.9 Hz, 2

H), 7.25–7.19 (m, 2 H), 6.90–6.84 (m, 4 H), 5.07 (s, 4 H), 4.61 (s, 4 H), 4.49 (pseudo-t, J = 1.9 Hz, 4 H), 4.24 (pseudo-t, J = 1.9 Hz, 4 H), 1.80 (s, 2 H) ppm. ^{13}C NMR (63 MHz, $CDCl_3$, 25°C): δ = 159.21, 140.63, 136.85, 133.28, 129.12, 127.52, 127.30, 120.98, 114.04, 112.64, 100.12, 91.74, 82.85, 72.99, 71.47, 70.21, 65.21 ppm. HRMS (MALDI/ESI): calcd. for $C_{42}H_{34}FeO_4$ $[M]^+$ 658.1802; found 658.1802.

Compound 21: An oven-dried 10 mL round-bottomed flask was flushed with argon and charged with **20** (15 mg, 22.8 µmol) in freshly distilled and deoxygenated THF (5 mL). To the mixture, NaH (60 % dispersion in mineral oil, 18.2 mg, 456 µmol) was added at –10 °C, and the resulting suspension was stirred for 20 min. Methanesulfonyl chloride (5.3 µL, 45.6 µmol) was then added at –10 °C. The reaction mixture was warmed to room temperature overnight. To the reaction mixture, LiBr (39.6 mg, 456 µmol) was added, and the reaction was stirred at room temperature for 2 h. After the reaction was finished, the reaction mixture was poured onto water and extracted with EtOAc (2 × 50 mL). The organic phase was washed with water (2 × 50 mL) and brine (50 mL), dried with $MgSO_4$, filtered, and concentrated under reduced pressure. The crude product was purified by silica gel FCC with DCM/cyclohexane (1:5) to elute the bisbromo adduct **22** (40 %), EtOAc/cyclohexane (1:5) was utilized to elute **21**, and EtOAc/cyclohexane (1:1) was used to wash out the starting material **20** (21 %). The solvent was removed under reduced pressure to afford **21** as an orange solid, yield 33 % (5.5 mg, 7.28 µmol). ^{1}H NMR (600 MHz, $CDCl_3$, 25°C): δ = 7.54–7.52 (m, 2 H), 7.51 (d, $^3J_{H,H}$ = 8.1 Hz, 2 H), 7.41–7.38 (m, 4 H), 7.37 (d, $^3J_{H,H}$ = 8.0 Hz, 2 H), 7.25–7.21 (m, 2 H), 6.90–6.85 (m, 4 H), 5.09 (s, 2 H), 5.08 (s, 2 H), 4.64 (s, 2 H), 4.49 (pseudo-t, J = 1.9 Hz, 2 H), 4.46 (pseudo-t, J = 1.8 Hz, 2 H), 4.44 (s, 2 H), 4.24 (pseudo-dt, J = 4.9, 1.9 Hz, 4 H) ppm. ^{13}C NMR (151 MHz, $CDCl_3$, 25°C): δ = 159.05, 158.94, 140.49, 137.43, 137.29, 136.47, 133.16, 133.16, 129.19, 128.99, 128.96, 127.40, 127.16, 120.95, 120.83, 113.96, 113.87, 112.58, 112.50, 91.76, 91.60, 82.65, 82.60, 72.87, 72.85, 71.26, 71.23, 70.06, 69.87, 67.12, 67.02, 65.12, 33.27 ppm. HRMS (ESI-TOF): calcd. for $C_{42}H_{33}BrFeO_3$ $[M]^+$ 720.0959; found 720.0956.

Ether-Bridged Macrocycle 1: An oven-dried 20 mL round-bottomed microwave vial was flushed with argon, charged with NaH (60 % dispersion in mineral oil, 10 mg, 251 µmol), **21** (5.5 mg, 7.2 µmol), and freshly distilled and deoxygenated THF (15 mL). The suspension was heated to70 °C for 2 h, after which MALDI MS indicated the complete consumption of the starting material. The reaction mixture was cooled to room temperature, transferred to an Erlenmeyer flask, and quenched by the dropwise addition of water (50 mL). The organic phase was eluted with ethyl acetate, washed with water (2 × 50 mL) and brine (50 mL), dried with $MgSO_4$, filtered, and concentrated under reduced pressure. The crude product was purified by silica gel column chromatography with EtOAc/cyclohexane (1:3). The solvent was removed under reduced pressure to afford the ether-bridged derivative **1** as an orange oil, yield 70 % (3.4 mg, 7.62 µmol). ^{1}H NMR (600 MHz, $CDCl_3$, 25°C): δ = 7.67 (d, $^3J_{H,H}$ = 7.9 Hz, 4 H), 7.50–7.44 (m, 6 H), 7.35–7.28 (m, 2 H), 7.01 (dd, $^3J_{H,H}$ = 8.3, $^4J_{H,H}$ = 1.1 Hz, 2 H), 6.96 (td, $^3J_{H,H}$ = 7.5, $^4J_{H,H}$ = 1.0 Hz, 2 H), 5.14 (s, 4 H), 4.61 (pseudo-t, J = 1.8 Hz, 4 H), 4.58 (s, 4 H), 4.30 (pseudo-t, J = 1.8 Hz, 4 H) ppm. ^{13}C NMR (151 MHz, $CDCl_3$, 25°C): δ = 159.22, 137.78, 136.60, 132.65, 129.04, 128.00, 127.21, 120.94, 114.02, 112.19, 92.06, 82.67, 72.52, 72.41, 70.62, 70.03, 65.82 ppm. HRMS (MALDI/ESI): calcd. for $C_{42}H_{32}FeO_3$ $[M]^+$ 640.1696; found 640.1696.

Compound 22: A 5 mL round-bottomed flask was dried with a heat gun, flushed with argon, and charged with **20** (50 mg, 756 umol) in freshly distilled and deoxygenated THF (5 mL). NaH (60 % dispersion in mineral oil, 152 mg, 37 mmol) was added, and the reaction mixture was stirred for 20 min. Methanesulfonyl chloride (58 µL, 152 µmol) was then added at –10 °C, and the reaction was warmed slowly to room temperature overnight. To the reaction mixture, LiBr (133 mg, 1.5 mmol) was added, and the reaction was stirred at room temperature for 2 h. After the completion of the reaction, the mixture was poured onto water and extracted with EtOAc (2 × 50 mL). The organic phase was washed with water (2 × 50 mL) and brine (50 mL), dried with $MgSO_4$, filtered, and concentrated under reduced pressure. The crude product was purified by filtration through a silica gel plug with DCM/cyclohexane (1:5). The solvent was removed under reduced pressure to afford **22** as an orange oil, which solidified upon standing at 4 °C, yield 69 % (41 mg, 0.052 mmol). ^{1}H NMR (400 MHz, $CDCl_3$, 25°C): δ = 7.51 (d, $^3J_{H,H}$ = 8.1 Hz, 4 H), 7.43–7.37 (m, 6 H), 7.26–7.20 (m, 2 H), 6.91–6.84 (m, 4 H), 5.08 (s, 4 H), 4.50 (pseudo-t, J = 1.9 Hz, 4 H), 4.45 (s, 4 H), 4.27 (pseudo-t, J = 1.9 Hz, 4 H) ppm. ^{13}C NMR (101 MHz, $CDCl_3$, 25°C): δ = 159.21, 140.63, 136.58, 133.28, 129.12, 127.52, 127.30, 120.98, 114.04, 112.64, 100.12, 91.74, 82.85, 72.99, 71.47, 70.21, 65.21 ppm. HRMS (MALDI/ESI): calcd. for $C_{42}H_{32}Br_2FeO_2$ $[M]^+$ 782.0113; found 782.0111.

Compound 23: A 5 mL round-bottomed flask was dried with a heat gun, purged with argon, and charged with vinylmagnesium bromide (0.7 M solution in THF, 1.5 mL, 1.04 mmol; clear, light brown solution) and CuI (10 mg, 52 umol), and the mixture was cooled to –78 °C. To the stirred suspension, **22** (41 mg, 52 umol) in freshly distilled and deoxygenated THF (5 mL) was added, and the mixture was allowed to reach room temperature overnight. After the reaction was complete, the suspension was poured onto a saturated aqueous NH_4Cl solution (100 mL) and extracted with EtOAc (2 × 50 mL). The combined organic phases were washed with water (2 × 50 mL) and brine (50 mL), dried with $MgSO_4$, and filtered, and the volatiles were removed under reduced pressure. The crude product was purified by silica gel FCC with DCM/cyclohexane (1:10). The solvent was removed under reduced pressure to afford **23** as an orange oil, yield 68 % (24 mg, 0.035 mmol). ^{1}H NMR (400 MHz, $CDCl_3$, 25°C): δ = 7.47 (d, $^3J_{H,H}$ = 8.0 Hz, 4 H), 7.41 (dd, J = 7.5, 1.7 Hz, 2 H), 7.25–7.18 (m, 6 H), 6.94–6.84 (m, 4 H), 5.94 (ddt, $^3J_{H,H}$ = 16.9, $^3J_{H,H}$ = 10.2 Hz, $^3J_{H,H}$ = 6.7 Hz, 2 H), 5.13–5.01 (m, 8 H), 4.49 (pseudo-t, J = 1.9 Hz, 4 H), 4.22 (pseudo-t, J = 1.9 Hz, 4 H), 3.37 (d, $^3J_{H,H}$ = 6.7 Hz, 4 H) ppm. ^{13}C NMR (63 MHz, $CDCl_3$, 25°C): δ = 159.21, 139.69, 137.37, 134.82, 133.18, 128.96, 128.73, 127.38, 120.77, 115.84, 113.97, 112.68, 91.68, 82.59, 72.80, 71.42, 70.32, 66.94, 39.94 ppm. HRMS (MALDI/ESI): calcd. for $C_{46}H_{38}FeO_2$ $[M]^+$ 678.2217; found 678.2215.

Macrocycle 2: An oven-dried 50 mL Schlenk flask was purged with argon and charged with a solution of **23** (20 mg, 295 µmol) in freshly distilled dichloroethane (27 mL) and a solution of the first-generation Grubbs catalyst (3.46 mg, 15 mol-%) in dichloroethane (3 mL). The reaction mixture was degassed with bubbling argon for 15 min. Then, the flask was closed with a rubber septum, and the mixture was heated to 70 °C for 16 h. After the reaction was complete, the mixture was cooled to room temperature and diluted with EtOAc (50 mL). The crude mixture was concentrated and purified by silica gel FCC with DCM/cyclohexane (1:10). The solvent was removed under reduced pressure to provide the macrocycle **2** as an orange solid (a mixture of *E* and *Z* isomers, 73:27), yield 57 % (11 mg, 0.017 mmol). The HSQC resolved ^{1}H–^{13}C spectra is shown in Figure S17. ^{1}H NMR (600 MHz, $CDCl_3$, 25°C): δ = 7.57–7.52 (m, 4 H, overlapping signals of *E*/*Z*), 7.47–7.42 (m, 2 H, overlapping signals of *E*/*Z*), 7.32–7.25 (m, 4 H, overlapping signals of *E*/*Z*), 7.02–6.97 (m, 2 H, overlapping signals of *E*/*Z*), 6.97–6.90 (m, 2 H, overlapping signals of *E*/*Z*), 5.73–5.65 (m, 2 H, overlapping signals of *E*/*Z*), 5.16–5.13 (m, 4 H, overlapping signals of *E*/*Z*), 4.63 (pseudo-t, J = 1.8 Hz,

4 H, *Z* isomer), 4.61 (pseudo-t, *J* = 1.9 Hz, 4 H, *E* isomer), 4.33 (pseudo-t, *J* = 1.8 Hz, 4 H, *Z* isomer), 4.29 (pseudo-t, *J* = 1.8 Hz, 4 H, *E* isomer), 3.54 (d, $^3J_{H,H}$ = 5.1 Hz, 4 H, *Z* isomer), 3.46–3.38 (m, 4 H, *E* isomer) ppm. ^{13}C NMR (151 MHz, $CDCl_3$, 25°C): δ = 127.22, 132.72, 128.98, 112.71, 121.00, 130.49, 129.07, 70.20, 72.51, 72.50, 72.51, 72.67, 33.37, 38.70 ppm; only proton-bound carbon atoms are reported. HRMS (MALDI/ESI): calcd. for $C_{44}H_{34}FeO_2$ $[M]^+$ 650.1904; found 650.1903.

Allyl Ether 24: A 100 mL round-bottomed flask was purged with argon and charged with **20** (30 mg, 0.045 mmol), which was dissolved in freshly distilled THF (50 mL). To the stirred solution, NaH (7.28 mg, 0.18 mmol) was added in one portion at room temperature. After no more gas was produced, allyl bromide (0.016 mL, 0.182 mmol) was added to the mixture, which was then heated to 60 °C for 5 h. After the reaction was complete, the mixture was quenched with water (50 mL) and washed with $NaHCO_3$ (50 mL) and brine (75 mL). The organic layer was dried with Na_2SO_4, filtered, and concentrated under reduced pressure. The crude product was purified by silica gel column chromatography with EtOAc/cyclohexane (1:5). The solvent was removed under reduced pressure to afford **24** as an orange solid, yield 60 % (20 mg, 0.027 mmol). ^{1}H NMR (400 MHz, $CDCl_3$, 25°C): δ = 7.54–7.49 (m, 4 H), 7.42–7.38 (m, 2 H), 7.38–7.34 (m, 4 H), 7.25–7.19 (m, 2 H), 6.91–6.83 (m, 4 H), 5.93 (ddt, $^3J_{H,H}$ = 17.2, $^3J_{H,H}$ = 10.4 Hz, $^3J_{H,H}$ = 5.6 Hz, 2 H), 5.29 (dq, $^3J_{H,H}$ = 17.3, $^4J_{H,H}$ = 1.7 Hz, 2 H), 5.19 (dq, $^3J_{H,H}$ = 10.4, $^4J_{H,H}$ = 1.3 Hz, 2 H), 5.11 (s, 4 H), 4.52–4.47 (m, 8 H), 4.24 (pseudo-t, *J* = 1.9 Hz, 4 H), 3.99 (pseudo-dt, *J* = 5.6, *J* = 1.4 Hz, 4 H) ppm. ^{13}C NMR (63 MHz, $CDCl_3$, 25°C): δ = 159.10, 137.91, 136.46, 134.73, 133.18, 128.95, 127.86, 127.16, 120.82, 117.12, 113.97, 112.67, 91.67, 82.65, 72.84, 71.84, 71.34, 71.10, 70.18, 67.04 ppm. HRMS (MALDI/ESI): calcd. for $C_{48}H_{42}FeO_4$ $[M]^+$ 738.2428; found 738.2425.

Allyl Ether Macrocycle 3: An oven-dried 100 mL Schlenk flask was purged with argon and charged with a solution of allyl ether **24** (29 mg, 393 μmol) in freshly distilled and deoxygenated dichloroethane (29 mL) and a solution of the first-generation Grubbs catalyst (2.4 mg, 7.5 mol-%) in dichloroethane (3 mL). The reaction mixture was degassed with bubbling argon for 15 min. Then, the flask was closed with a rubber septum and heated to 70 °C overnight. After the reaction was complete, the mixture was cooled to room temperature, concentrated, and purified by silica gel column chromatography with EtOAc/cyclohexane (1:5). The solvent was removed under reduced pressure to afford **3** as an orange solid (a mixture of *E* and *Z* isomers, 73:27), and the isomers were separated by HPLC (silica 100 Å, 2-propanol/hexane 95:5, isocratic elution at 8 mL/min), yield 57 % (16 mg, 0.027 mmol). The HSQC- and HMQC-resolved spectra are shown in Figure S19. (*E*)-**3**: ^{1}H NMR (600 MHz, $CDCl_3$, 25°C): δ = 7.58 (d, $^3J_{H,H}$ = 7.8 Hz, 4 H), 7.44 (dd, $^3J_{H,H}$ = 7.6, 1.7 Hz, 2 H), 7.42–7.39 (m, 4 H), 7.30–7.26 (m, 2 H), 6.97 (pseudo-d, $^3J_{H,H}$ = 8.4 Hz, 2 H), 6.93 (pseudo-t, $^3J_{H,H}$ = 7.5 Hz, 2 H), 5.90–5.85 (m, 2 H), 5.09 (s, 4 H), 4.56 (s, 4 H), 4.55 (pseudo-t, *J* = 1.9 Hz, 4 H), 4.21 (pseudo-t, *J* = 1.8 Hz, 4 H), 4.08–4.04 (m, 4 H) ppm. ^{13}C NMR (151 MHz, $CDCl_3$, 25°C): δ = 127.29, 132.98, 127.71, 129.05, 112.37, 120.96, 129.53, 69.38, 71.78, 72.47, 69.94 ppm; only proton-bound carbon atoms are reported. (*Z*)-**3**: ^{1}H NMR (600 MHz, $CDCl_3$, 25°C): δ = 7.50 (d, $^3J_{H,H}$ = 7.8 Hz, 4 H), 7.37–7.33 (m, 2 H), 7.29 (d, $^3J_{H,H}$ = 7.8 Hz, 4 H), 7.24–7.20 (m, 2 H), 6.87 (pseudo-d, $^3J_{H,H}$ = 8.3 Hz, 2 H), 6.84 (pseudo-t, $^3J_{H,H}$ = 7.5 Hz, 2 H), 5.80–5.77 (m, 2 H), 5.03 (s, 4 H), 4.52–4.48 (m, 4 H), 4.43 (s, 4 H), 4.23–4.18 (m, 4 H), 3.94 (d, $^3J_{H,H}$ = 4.2 Hz, 4 H) ppm. ^{13}C NMR (151 MHz, $CDCl_3$, 25°C): δ = 127.32, 133.04, 128.05, 112.50, 120.90, 129.73, 70.17, 72.61, 71.68, 71.21, 65.06 ppm; only proton-bound carbon atoms are reported. HRMS (MALDI/ESI): calcd. for $C_{46}H_{38}FeO_4$ $[M]^+$ 710.2115; found 710.2113.

Structure Determination by Single-Crystal X-ray Analysis: The intensity data for suitably sized crystals of (*Z*)-**3** with the formula $C_{46}H_{38}Fe_1O_4$, *M* = 710.65 g were collected with a Stoe StadiVari diffractometer at 123 K by using Ga-K_α radiation with λ = 1.34143 Å. The STOE X-AREA suite was used for data collection and integration. The structure of (*Z*)-**3** was solved by the charge-flipping method by using the program Superflip to reveal the atomic positions. Least-squares refinement against *F* was performed for all non-hydrogen atoms with the program CRYSTALS, and Chebychev polynomial weights were used to complete the refinement. Plots were produced with Mercury. The X-ray crystallographic parameters as well as details of the data collection and structure refinement are presented in Table S1.

CCDC 1453128 for [(*Z*)-**3**] contains the supplementary crystallographic data for this paper. These data can be obtained free of charge from The Cambridge Crystallographic Data Centre.

Supporting Information (see footnote on the first page of this article): crystallographic data, NMR spectra (^{1}H, ^{13}C, HSQC, and HMQC), elemental analysis, and MS (EI-MS, HR-ESI-MS, and HR-ESI-MALDI) spectra.

Acknowledgments

The authors thank the Swiss National Science Foundation (SNF) (grant number 200020-159730) for continuous and generous financial support.

Keywords: Synthesis design · Ring-closing metathesis · Metallocenes · Macrocycles

[1] T. J. Kealy, P. L. Pauson, *Nature* **1951**, *168*, 1039–1040.
[2] G. Wilkinson, M. Rosenblum, M. C. Whiting, R. B. Woodward, *J. Am. Chem. Soc.* **1952**, *74*, 2125–2126.
[3] M. S. Driver, J. F. Hartwig, *J. Am. Chem. Soc.* **1996**, *118*, 7217–7218.
[4] R. Deschenaux, J. Santiago, *Tetrahedron Lett.* **1994**, *35*, 2169–2172.
[5] C. Engtrakul, L. R. Sita, *Organometallics* **2008**, *27*, 927–937.
[6] K. Di Gleria, M. J. Green, H. A. O. Hill, C. J. McNeil, *Anal. Chem.* **1986**, *58*, 1203–1205.
[7] Q. Lu, C. Yao, X. Wang, F. Wang, *J. Phys. Chem. C* **2012**, *116*, 17853–17861.
[8] T. Muraoka, K. Kinbara, Y. Kobayashi, T. Aida, *J. Am. Chem. Soc.* **2003**, *125*, 5612–5613.
[9] W. Y. Lee, C. H. Park, Y. D. Kim, *J. Org. Chem.* **1992**, *57*, 4074–4079.
[10] S. Höger, *Liebigs Ann./Recueil* **1997**, 273–277.
[11] J. E. Baldwin, *J. Chem. Soc., Chem. Commun.* **1976**, 734–736.
[12] D. R. Buckle, C. J. M. Rockell, *J. Chem. Soc. Perkin Trans. 1* **1985**, 2443–2446.
[13] P. Babin, J. Dunogues, M. Petraud, *Tetrahedron* **1981**, *37*, 1131–1139.
[14] R. Sterzycki, *Synthesis* **1979**, 724–725.
[15] J. Claffey, H. Müller-Bunz, M. Tacke, *J. Organomet. Chem.* **2010**, *695*, 2105–2117.
[16] N. M. Jenny, M. Mayor, T. R. Eaton, *Eur. J. Org. Chem.* **2011**, 4965–4983.
[17] J. Li, P. Huang, *Beilstein J. Org. Chem.* **2011**, *7*, 426–431.
[18] J. K. Pudelski, M. R. Callstrom, *Organometallics* **1994**, *13*, 3095–3109.
[19] I. R. Butler, S. B. Wilkes, S. J. McDonald, L. J. Hobson, A. Taralp, C. P. Wilde, *Polyhedron* **1993**, *12*, 129–131.
[20] T. Hundertmark, A. F. Littke, S. L. Buchwald, G. C. Fu, *Org. Lett.* **2000**, *2*, 1729–1731.
[21] M. S. Inkpen, A. J. P. White, T. Albrecht, N. J. Long, *Chem. Commun.* **2013**, *49*, 5663–5665.
[22] Y. He, M. Johansson, O. Sterner, *Synth. Commun.* **2004**, *34*, 4153–4158.

[23] G. Cahiez, O. Gager, A. Moyeux, T. Delacroix, *Adv. Synth. Catal.* **2012**, *354*, 1519–1528.
[24] F. Derguini-Boumechal, G. Linstrumelle, *Tetrahedron Lett.* **1976**, *17*, 3225–3226.
[25] R. Rossi, A. Carpita, M. G. Quirici, C. A. Veracini, *Tetrahedron* **1982**, *38*, 639–644.
[26] X. Lou, J. L. J. van Dongen, E. W. Meijer, *J. Am. Soc. Mass Spectrom.* **2011**, *21*, 1223–1226.
[27] J. D. Winter, G. Deshayes, F. Boon, O. Coulembier, P. Dubois, P. Gerbaux, *J. Mass Spectrom.* **2011**, *46*, 237–246.

Received: February 12, 2016
Published Online: April 5, 2016

